Cold temperature represses daily rhythms in the liver transcriptome of a stenothermal teleost under decreasing day length

Jenni M. Prokkola[a,d]*, Mikko Nikinmaa[a], Mario Lewis[a], Katja Anttila[a], Mirella Kanerva[a], Kaisa Ikkala[a], Eila Seppänen[c], Irma Kolari[c], Erica H. Leder[ab]

[a]Department of Biology, University of Turku, FI-20014, Finland

[b]Natural History Museum, University of Oslo, Oslo, NO-0318, Norway

[c]Natural Resources Institute Finland (Luke), Laasalantie 9, FI-58175 Enonkoski, Finland

[d]University of Eastern Finland, P.O. Box 111, FI- 80101 Joensuu, Finland

Keywords: salmonid, circadian rhythms, global warming, genomics, photoperiod

*Contact: jmprok@utu.fi, orcid.org/0000-0003-2987-4417

Summary statement:

Transcriptomic profiling of liver tissue in a cold-adapted fish suggests tight coupling of temperature responses and daily rhythms.

Abstract

The climate change -driven increase in temperature is occurring rapidly and decreasing the predictability of seasonal rhythms at high latitudes. It is therefore urgent to understand how a change in the relationship between the photoperiod and temperature can affect ectotherms in these environments. We tested whether temperature affects daily rhythms of transcription in a cold-adapted salmonid using high-throughput RNA-sequencing. Arctic char (*Salvelinus alpinus*) from a subarctic population were reared at a high and a low temperature (15°C and 8°C) for one month under natural, decreasing day length during late summer. Liver transcriptomes were compared between samples collected in the middle and towards the end of the light period and in the middle of the dark period. Daily variation in transcription was lower in fish from the low temperature compared to strong daily variation in warm-acclimated fish, suggesting cold temperatures dampen the cycling of transcriptional rhythms under a simultaneously decreasing day length. Different circadian clock genes had divergent expression patterns, responding either by decreased expression or by increased rhythmicity at 15°C compared to 8°C. The results point out mechanisms that can affect the ability of fish to adapt to increasing temperatures caused by climate change.

Introduction

In the strongly seasonal habitats in high latitudes, organisms anticipate seasonal changes in temperature by tracking daily and annual variation in photoperiod (Wood & Loudon 2014). Photoperiod regulates the central circadian clock, an oscillating transcriptional feedback loop located in mammals in the suprachiasmatic nucleus of the hypothalamus, and in fish in the pineal gland, although in fish the peripheral clocks may be more independent (Idda *et al.* 2012; Lowrey & Takahashi 2004). The central clock acts as a master regulator of the rhythms of peripheral tissues (Idda *et al.* 2012; Lowrey & Takahashi 2004), but in addition to central clock entrainment, nutrient and redox status and other factors can also entrain the clock (Asher *et al*. 2011; Yang *et al*. 2006), and in fish the peripheral rhythms can be directly light-entrained (Whitmore *et al.* 2000). Across tissues, transcriptional regulation is a central feature of circadian rhythms (Akhtar *et al.* 2002; Doherty & Kay 2010). However, the genes under circadian control are tissue-specific (Panda *et al*. 2002).

Besides photoperiod, temperature can regulate circadian rhythms. In a temperate fish, the Atlantic salmon (*Salmo salar*), acclimation at a warm temperature can increase melatonin secretion during the dark phase (Porter *et al.* 2001), and in zebrafish (*Danio rerio*), temperature bouts and daily cycles can entrain the clock (Lahiri et al. 2005; Lahiri et al. 2014; Lopez-Olmeda & Sanchez-Vazquez. 2009). On the other hand, temperature compensation within an ecologically relevant temperature range is important for an endogenous clock in order to maintain a *ca*. 24-h period length, particularly in ectotherms (Brown *et al.* 1948). However, the mechanism by which this is achieved and whether the clocks of cold-adapted species conform to this principle is not well known.

Deeper insight into the biological clocks of species at high latitudes is now highly warranted, as the temperature increase and extreme weather events associated with climate change can introduce a mismatch between an organism's circannual clock and the environmental conditions, which is likely to have negative impacts on wild populations

(Jorgensen & Johnsen 2014; Stevenson *et al.* 2015). Particularly in ectotherms, increasing temperature could also lead to changes in circadian rhythms within seasons. Adverse climatic effects are especially emphasized in the Arctic (Marshall *et al.* 2014) and projections of climate change over the next decades show warming in the Arctic will likely be strongest during the autumn and winter (Walsh 2008). As circadian variation in transcription can mask the responses to temperature for many genes (Podrabsky & Somero 2004), accounting for daily variation in gene expression studies can also lead to major improvements in understanding the mechanisms affecting temperature tolerance. This has particular importance for research on stenothermal species that do not cope well at high temperatures and whose adaptive responses we need to understand better, such as the Arctic char (Anttila *et al*. 2015; Jeuthe *et al.* 2015; Penney *et al*. 2014).

In plants, cold temperatures have a direct input into the circadian machinery to repress processes that would otherwise be triggered by seasonal photoperiod changes, such as flowering (Mizuno *et al*. 2014). Arctic ectotherms would also likely experience a maladaptive response if only photoperiod was involved in signalling life-history events. Therefore we tested if cold temperature during a period of late summer photoperiod would result in a different pattern of transcript expression compared to warm temperature, particularly with respect to transcripts that have a daily rhythm. Consequently, our hypothesis was that temperature affects transcriptional rhythmicity in a stenothermal fish during late summer day lengths that coincide with the annual temperature maximum in the wild. To our knowledge this is the first study evaluating temperature effects on overall transcriptional rhythms of a mostly Arctic species. Therefore, the results form a starting point to more detailed and ecologically relevant studies.

Materials and methods

Study site and fish

The population of Arctic char used in the experiments originated from Lake Kuolimo, Finland (61°16′ N; 27°32′ E). The experiments were conducted at the Natural Resources Institute Finland (Luke) in Enonkoski, Eastern Finland in 2013. Year-old Arctic char from a brood stock that has been maintained at the aquaculture facilities for three generations were reared in natural light-dark rhythm and ambient temperature (approximately 8°C before the acclimations) using water fed from Lake Pahkajärvi (62°04′ N; 28°33′ E) prior to the experiment. In early July, warm acclimation was initiated by transferring fish to a tank that was heated to 15°C (mean 14.9 ± 0.6°C) over one day, while another group of fish was maintained at a cold temperature (mean 7.7 ± 0.2°C, from hereon 8°C). The test temperatures were roughly at the low- and high-end of the temperatures experienced and tolerated by the fish during summer; the cold water was the coldest available in the lake in the summer, and negative consequences for fish health from temperatures higher than 15°C had previously been found in the hatchery. Notably, the temperature range 8-15°C can occur simultaneously at different depths in lakes populated by Arctic char. There was no daily variation in water temperature in either group. The acclimations were conducted under natural light conditions, the length of light period being 19 h 20 min at the beginning and 17 h 15 min at the end of the acclimation period. No artificial lighting was provided for the fish, instead all light entered through windows located on two sides of the room. The tanks were not exposed to direct sunlight. Fish were acclimated in identical, round, approximately 320 L flow-through tanks. Oxygen levels were kept above 80% air-saturation throughout the acclimations, and temperatures of the tanks were monitored and adjusted daily. Mean O_2 levels during acclimation were 10.2 ± 2.3 mg/L in the warm treatment and 12.5 ± 2.3 mg L^{-1} in the cold treatment. Thus, we minimized random variation between the two tanks by using controlled

conditions (feeding, oxygen level, density and size of fish, uniform photoperiod and light intensity, removal of uneaten food and faeces). Fish were fed with commercial fish pellets (Raisio Group; www.raisiogroup.com) *ad libitum* using automatic feeders and fasted for 24 h before sampling.

After the four-week acclimation, fish from each temperature were collected at three time points during the day; at 12:30 (middle of the light period), 20:30 (approx. 1 h before sunset) and at 01:30 (middle of the dark period), hereafter referred to as day, evening and night, euthanized with 200 ppm sodium bicarbonate-buffered tricaine methanesulfonate (MS-222), then measured and weighed. Blood was collected in heparinized capillary tubes for haematocrit measurements. Liver tissue was removed and flash frozen in liquid nitrogen, after which the samples were stored at –80°C until analysis. The fish were sexed during the dissection by inspecting the gonads. The handling time for each fish from euthanasia to removal of tissue was <3 min.

RNA extraction, library preparation and sequencing

Three males per each time point-temperature combination with roughly uniform size (average body mass, 15°C = 22.2 ± 8.4 g (SD), 8°C = 24.2 ± 10.4 g, average fork length at both temperatures = 13.7 ± 1.8 cm) were selected for RNA extraction and sequencing (total N=18). These fish also had uniform haematocrit values (47 ± 4 % and 46 ± 5% at 8°C and 15°C, respectively). RNA was extracted from approximately 10 mg liver tissue at the University of Turku. Extractions were performed using Tri-Reagent (Molecular Research Center) following the manufacturer's protocol. In short, tissue was homogenized using TissueLyser (Qiagen) for 90 s at 30 Hz speed. Eluted RNA was treated with DNase I and purified with a re-extraction using Tri-Reagent. RNA was quantified using NanoDrop 2000 spectrophotometer (Thermo Scientific) and its integrity was confirmed using 2100 Bioanalyzer (Agilent) (average RNA integrity number 9.95). Strand-specific cDNA library preparation and sequencing were

conducted at Beijing Genomics Institute (BGI Hong Kong) using TruSeq RNA Sample Prep

Kit v2 (Illumina) and Illumina HiSeq2000 instrument. The reads were trimmed from adapter

sequences at the sequencing facility. We checked the sequencing data for quality with

FastQC, and trimmed reads using Trimmomatic (details in Supplemental Information).

De novo *transcriptome assembly and differential expression analysis*

The whole genome sequence of Arctic char is not yet available; thus, a *de novo* transcriptome

assembly was generated from quality-trimmed paired-end (PE) reads using Trinity, v.2.0.6

(Grabherr *et al.* 2011) (details in Supplemental Information). The trimmed PE reads from all

samples were aligned against the assembly using Bowtie2, ignoring discordant and mixed

alignments and allowing a maximum of 40 multiple alignments per read. Read counts per

cluster were obtained from generated alignment files using Corset (Davidson & Oshlack

2014). Clusters that were expressed with >1 counts per million reads (cpm) in at least three

samples across all 18 samples were included in the analysis, and are hereafter referred to as

genes, although some of the assembled sequences may not correspond to actual mRNAs, but

instead to long non-coding or pre-mRNAs. Reads for gene isoforms and paralogs of high

similarity may be counted under the same clusters, but this issue remains challenging to

circumvent in a *de novo* assembly analysis. The assembly was filtered to include only the

transcripts of expressed genes to generate a final assembly available for download.

DE analysis was conducted using the limma package v.3.28.21 (Ritchie *et al.* 2015;

Smyth 2005) in RStudio, v. 0.99.903 (R v. 3.3.1, R Core Team 2016). The data were

normalized for library sizes using edgeR package TMM-normalization (Robinson & Oshlack

2010). The voom method was applied to obtain precision weights for the mean-variance

relationships of expression levels (Law *et al.* 2014) that were included in the limma empirical

Bayes analysis pipeline (Ritchie *et al.* 2015; Smyth 2005). We built four contrast matrices for

DE analysis including 1) the average temperature effect across time points, 2) pairwise

differences between time points within temperatures, 3) The interaction effect of time point and temperature and 4) differences between temperatures within time points. The average effects of time points were not included in the analysis due to the strong temperature-dependence of the effect. The probability (p) values were adjusted for false discovery rate (FDR) using the Benjamini-Hochberg method and adjusted p-value 0.05 was used as the significance threshold, calculated using limma decideTest method "global" across contrasts in matrices 2 and 4 to compare the strengths of different contrasts.

To evaluate the proportion of total variation between samples explained by time or temperature, the voom-transformed and normalized read counts were further used in partial redundancy analysis (RDA) using package vegan v. 2.4-3 (Oksanen *et al.* 2017). Variation between samples was explained, first, by time, temperature and their interaction, second, by time after conditioning for the effect of temperature and third, by temperature after conditioning the effect of time. Clustering of samples was visualized using scaling based on genes.

The normalized $\log_2$ cpm data generated by voom for selected target genes were visualized using packages plyr, ggplot2 and gplots in R (Warnes *et al*. 2016; Wickham 2009; Wickham 2011). R codes used in the analysis and visualization of read counts are provided in Supplemental Material.

Transcriptome annotation

Open reading frame (ORF) peptide sequences were obtained for transcripts in the final assembly using the TransDecoder software. The predicted ORFs were annotated with three databases using Basic Local Alignment Search Tool for proteins (BLASTp v.2.2.31). All of the predicted ORF sequences were annotated with predicted zebrafish (downloaded Oct 24 2015 from Ensembl) and salmon (NCBI *Salmo salar* Annotation Release 100) proteins using a reciprocal best hits approach and an e-value cutoff 1×10^{-5}. Additionally, the ORFs were

annotated with NCBI non-redundant protein database (downloaded Nov 25th 2015) with e-value cutoff 1×10^{-5} and when the query sequence matched the target sequence at >50 % protein length. The annotations were prioritized with the order zebrafish > salmon > NCBI nr. When available, gene descriptions were retrieved from Ensembl using biomaRt in R. Gene symbols were retrieved for zebrafish Ensembl IDs, salmon Refseq IDs and NCBI gene names using Biological DataBase Network (https://biodbnet-abcc.ncifcrf.gov). Annotations were retrieved for 9,491, 4,037 and 4,117 genes with zebrafish peptides, Atlantic salmon predicted peptides and the NCBI nr-database, respectively. In total, 20,394 out of 44,784 ORFs in the assembly (45.5%) were annotated with 18,013 unique protein IDs.

Because only a limited proportion of the annotations retrieved for the transcripts could be transformed into human IDs for further analyses, we also annotated all ORF peptide sequences with human peptide sequences using BLASTp v.2.4.0 with an E-value threshold 10^{-5}. After identifying human orthologs, we supplemented the annotation by the previously obtained gene symbols for genes that were missing an annotation. In total 18,232 genes were annotated using this approach with 9,577 unique gene symbols.

Weighed correlation network analysis and upstream regulator analysis

In order to investigate patterns of co-expression among transcripts, we also analyzed the normalized, voom transformed data using weighed correlation network analysis (WGCNA) (Langfelder & Horvath 2008). We first removed transcripts with low variation across treatments (cpm variance < 1) and ran the function blockwiseModules to identify potentially co-regulated genes. We created a signed network using a soft thresholding power 20, minimum module size of 30 transcripts, and a merge cut height of 0.25. As it is likely that modules of genes are regulated by common transcription factors, we examined the annotated members of the ten modules that were significantly correlated with temperature treatment or time using the upstream regulator analysis in the Ingenuity Pathway Analysis (IPA) software

(Qiagen), This analysis uses a Fisher's Exact Test to determine whether the input list has significantly more members that are known targets of transcription factors than a random list of genes.

Results

De novo *assembly quality*

We obtained on average 40.1 ± 6.5 (SD) million, min 27.3 million and max 60.6 million, raw PE reads per sample for the DE analysis. 99% of reads passed quality trimming and were used in the assembly and read alignment. The assembly contained approximately 210,000 transcripts prior to and 88,487 transcripts after filtering based on expression values. The transcripts originated from approximately 42,000 genes. The alignment rate of reads was on average $23.0 \pm 6.0\%$ unique and $60.3 \pm 1.2\%$ multiple aligned reads. Inspection of sam-files generated by Bowtie2 revealed that multiple aligned reads were generally aligning to different isoforms of the same Trinity genes, thus having small effect on the gene-level expression analysis. Since determining isoform-specific expression accurately was not possible due to the short read length and presence of multiple paralogous genes (as a result of a salmonid-specific whole genome duplication event (e.g., Macqueen & Johnston 2014)), we focused on the gene-level differences in the DE analysis. However, many conserved gene paralogs of salmonids were found as separate transcripts or genes in the assembly (Table S1). BUSCO analysis using conserved, near-universal single-copy orthologs (Simao *et al.* 2015) indicated that the assembly had 61% completeness, 4.7% fragmentation and 33% missing orthologs of these genes. The transrate (Smith-Unna *et al.* 2016) score of the assembly was increased by expression-level filtering from 0.18 to 0.24.

Daily rhythms in gene expression were repressed at 8°C compared to 15°C

Clustering of samples using partial RDA showed the samples from different temperatures could be clearly separated by their pairwise distances (Fig. 1A), and that much larger distances separated samples from different time points at 15°C than at 8°C after conditioning for the effect of temperature (Fig. 1A). Likewise, the samples were clearly separated between temperatures after conditioning for the effect of time, with day and evening samples clustering together within time points (Fig. 1C). In the DE analysis, we found significant pairwise differences between time points in 2,080 genes at 15°C (Table S2), representing *ca*. 5 % of the whole transcriptome, while 41 genes showed temporal variation at 8°C (Table S3), only five of which were annotated. Nine genes showed temporal variation at both temperatures (two annotated: *filamin A interacting protein 1-like* and *zinc finger protein 2-like*). At 15°C, the differences in gene expression between time points were the largest between the day and evening, and the direction of change from day to evening or night was for the most part an increase in expression (Table 1, Table S2, Fig. S1). In addition, we found 2,925 genes showing a significant time-temperature interaction effect (Table S4).

Circadian clock genes respond to temperature

We detected differential expression in two orthologs of *circadian locomotor output cycles kaput 1's* (*clock1*). A comparison of the cDNA sequences of *clock* genes across vertebrates revealed one of the *clock* transcripts to be more similar to *clock1a* (Cluster-92957.0), while the other one was more similar to *clock1b* (Cluster-78073.3); it is referred to as *clock1b* from hereon. *Clock1a* (Fig. S2a), as well the orthologs of *aryl hydrocarbon receptor nuclear translocator-like protein 2* (*arntl2*, a.k.a *bmal/cycle2)* and *cryptochrome 1aa* (*cry1aa*) were

more highly expressed at 8°C than at 15°C. *Clock1b* was expressed less, and *arntl1* expressed more, during the night and evening than during the day at 15°C (Fig. S2b-c). We additionally compared the differentially expressed genes to those from "BMAL1-CLOCK,NPAS2 activates circadian gene expression" super pathway in Path Cards, a pathway unification database (http://pathcards.genecards.org) (Belinky *et al*. 2015), which lists 78 genes that includes the core clock components and their interaction partners. In total, we found that 36 members of this pathway were significantly differentially expressed between time points, temperatures or in interaction of the two (Table 2).

Transcriptome differences between temperatures were the largest in the evening

We contrasted the average effect of temperature across all time points in the DE analysis, which resulted in 4,099 genes with higher expression in the warm than in the cold treatment, and 4,633 genes with higher expression in the cold than in the warm treatment with FDR < 0.05 (in total 20% of the transcriptome, Fig. S3, Table S4). However, when comparing temperatures in each time point independently, the number of differentially expressed genes varied greatly (Fig. 2). Only 176 genes that were differentially expressed between temperatures were shared across all time points.

Gene modules identify regulatory links between temperature responses and the circadian clock

WGCNA clusters genes with similar patterns of expression across samples to create modules of genes that are likely co-expressed. Since this method uses hierarchical clustering of expression values to group genes into modules, the connectivity of the genes in the modules could reflect the response to time, temperature or their interaction. After the modules were created, the correlation of the module genes with time and temperature was calculated to

examine the strength of the correlation of the module with a given trait. There were two modules that were significantly correlated with time and eight modules that were significantly correlated with temperature (Table 3), although since the clustering is independent of the traits, modules could also reflect the interaction between traits. Details of the genes belonging to the modules are provided in Table S6.

When the expression of the genes within the modules is visualized using heatmaps, the yellow module shows a very clear interaction between time and temperature with the genes from the cold acclimated individuals being uniformly expressed across all time points (with one outlier) and the warm acclimated individuals showing a clear time response (Fig. 3). The green, turquoise and blue modules also show this interaction to a large extent, but there is slightly more variation among individuals (Fig. S4-6). The brown module was mainly clustering genes that are responding to the temperature difference but had no daily rhythm (Fig. S7). Significantly expressed genes from the DE analysis also overlapped with many genes in the modules correlated with time or temperature, while only seven significant DE genes belonged to modules not significantly correlated with the traits (Table 4).

In the turquoise module, which was significantly correlated with temperature but contained many genes significant for time and time-temperature interaction, HNF4α was the top-scoring potential upstream regulator (Table S7). The expression of *hnf4α* was affected by time-temperature interaction (Fig. S2d). There were also 19 of the 78 genes from "BMAL1-CLOCK,NPAS2 activates circadian gene expression" super pathway identified as potential upstream regulators of the genes in this module, twelve of which were also significant in the DE analysis results (Table 2). In comparison, only five genes from this super pathway were found among the upstream regulators of the yellow module, which was primarily correlated with time, highlighting the temperature dependent effects of circadian regulators.

Discussion

The main finding in our study was the profound thermal effect on daily rhythms in transcription, which was observed during a season of decreasing day length. In invertebrates, very low temperatures can stop the circadian clock from cycling (Brown & Webb 1948; Hastings & Sweeney 1957) and in ectothermic vertebrates, low temperature can dampen circadian rhythms in melatonin secretion or clock gene expression (Rensing & Ruoff 2002; Vallone *et al*. 2007), but this study is the first to report genome-wide decrease in transcriptional rhythms due to the combination of decreasing day length and cold temperature in fish. However, in Arctic char, melatonin rhythm persists throughout the year, suggesting that the pineal gland functions also at cold temperatures (Strand *et al*. 2008). A potentially similar phenomenon, where transcriptional rhythms of circadian clock genes can be paused by cold treatment is known in plants (Martinocatt & Ort 1992). Therefore, we now have an indication that this response, where a decrease in temperature reduces or stops the cycling of specific transcripts, may be common for many different taxa. Having said the above, we note that a shift in the phase of the daily rhythm instead of decrease is amplitude may explain the results for at least some of the genes. However, this alternative is, in our opinion, less likely in the context of previous studies in other organisms (see above), and we would expect to see more genes showing significant fold-changes between time points at 8°C if the phase shift explained the majority of the findings. Our results also highlight that daily variation should be taken into consideration in future studies that apply genomics techniques to uncover adaptive responses, supporting previous observations (Tauber & Kyriacou 2007).

Large daily variation in transcription and in other processes can be mediated by endocrine signalling, as outlined in Cowan et al. (2017) for fishes. For instance, melatonin may affect the temperature-dependent transcriptional rhythms that we observed, for it plays a

role in circadian regulation and warm temperature can increase night time melatonin secretion, as demonstrated in Atlantic salmon and white sucker (*Catostomus commersoni*) (Porter *et al.* 2001; Zachmann *et al.* 1992). Further, activity of the melatonin synthesis-limiting enzyme of teleosts, arylalkylamine N-acetyltransferase 2 (AANAT2), is correlated with the preferred temperature in a range of fishes, suggesting that there is an adaptive relationship between temperature and melatonin synthesis (Falcon *et al*. 2009). Other metabolic and endocrine responses may also play a role and can have joint effects on the temperature-dependent rhythms we observed. However, it is also possible that the effects on liver transcriptional rhythms are independent of the pineal gland, because melatonin secretion in Arctic char seems to occur also in cold (Strand *et al.* 2008).

In ectotherms, core clock gene expression shows changing amplitudes and peaks, but a conserved period length of 24 h, across temperatures (Kidd *et al.* 2015; Lahiri *et al.* 2005; Rensing & Ruoff 2002), or a universal increase, accompanied by dampening of rhythms (Vallone *et al*. 2007). Likewise, cold temperature can dampen transcriptional rhythms in clock genes in *Arabidopsis thaliana*, a plant model species (Bieniawska *et al*. 2008). Our results showed that transcription of none of the core clock genes showed daily variation at 8°C, while two of them were rhythmic at 15°C (*clock1b, arntl1*), and five of them (*clock1a, arntl1, arntl2, cry1aa, per1*) were more highly expressed at 8°C than at 15°C. Thus, the different clock genes may have divergent roles in integrating the thermal responses with circadian rhythms. *Clock*, *arntl* and *cry* are conserved members of the vertebrate circadian clock feedback loop, which oscillates in peripheral tissues and in the central clock with a 24-h rhythm. *Cry* transcription, along with the clock gene *period* and hundreds of other genes, is regulated by CLOCK and ARNTL binding on E-box elements, and the accumulation of PERIOD and CRY proteins gradually inhibits the DNA binding of CLOCK and ARNTL (Lowrey & Takahashi 2004). In teleosts, different paralogs of circadian clock genes can have diverged roles in the feedback loop, as shown in zebrafish (Vatine *et al*. 2011). To our knowledge, there is no previous research on clock gene expression in Arctic char. Although it

is unclear how temperature acts to repress the core clock components and how their protein levels are affected, it is likely that the lack or decrease of daily cycling of many downstream genes is the result of repressed rhythmicity of these core regulators, as studies in mice have identified thousands of clock-controlled genes in the liver tissue (Yoshitane *et al*. 2014). In future studies, comparing CLOCK protein accumulation at different acclimation temperatures and across populations with different thermal histories would be useful for understanding how it can trigger pathways related to shifts in life-history traits. CLOCK may be associated with seasonal regulation; the gene was found in a quantitative trait locus region associated with reproduction and growth in salmonids (Leder *et al.* 2006; Paibomesai *et al.* 2010) and *clock* alleles have a latitudinal gradient in the Chinook salmon (*Oncorhynchus tshawytscha*) and the blue tit (*Cyanistes caeruleus*) (Johnsen *et al.* 2007; O'Malley & Banks 2008).

Due to the small sample size for each time point in this study, the statistical analysis likely somewhat suffered from low power to detect differences between time points using the pairwise contrasts. However, the partial RDA and WGCNA support the conclusions of DE analysis. Both analyses indicated clear interaction between temperature and daily rhythms in regulating gene expression, with more pronounced changes at 15°C compared to 8°C. These changes could be mediated by transcriptional upstream regulators. Upstream analysis of the WGCNA module genes notably showed hepatocyte nuclear factor 4α (HNF4α) was among the most significant upstream regulators of most of the modules tested in IPA. HNF4α binds to the promoters of almost half of the genes occupied by RNA polymerase II in human hepatocytes (Odom *et al*. 2004). It is a likely candidate for mediating the signalling between thermal (metabolic) regulation and the circadian clock, since disrupted light-dark cycles alter the transcription of HNF4α, as well as other hepatic gluconeogenic regulatory genes in mice (Oishi and Itoh, 2013). In our data, *hnf4α* expression was time-dependent in contrasting directions at different temperatures (Fig. S2d).

Our gene expression data can provide new insights into the molecular mechanisms linking circadian regulation of transcription to an organismal response such as hypoxia and

temperature tolerance in fish. Notably, we have previously shown that Arctic char acclimated to similar temperatures as in the present study have significant differences in thermal tolerance, indicating physiological acclimation to the temperature treatments (Anttila *et al.* 2015). Further, understanding how temperature affects the patterns of daily variation in transcriptome expression can advance the development of chronotherapeutic approaches to treating fish diseases, as the toxicity of therapeutic agents, such as H_2O_2, can be rhythmic (Vera *et al.* 2016). For instance, based on transcriptional patterns, daily variation in drug hepatotoxicity is expected to be low at relatively cold temperatures, but could vary throughout the day at warmer temperatures.

Conclusions

We found daily rhythms in gene expression were dampened at 8°C but strong at 15°C in Arctic char, which suggests daily transcriptional rhythms are strongly affected by temperature in this species, and leads to new hypotheses on the role of temperature in the regulation of biological clocks in fish. Firstly, the temperature compensation feature of circadian rhythms may have been under stronger selection in eurythermal than in stenothermal species, which generally experience small variation in temperature. Experiments on both steno- and eurythermal species under constant conditions at different temperatures could be used to address this. Secondly, temperature-dependent changes in the clock machinery may be induced by or enhance the negative effects of cold temperature on metabolic rate, because the circadian system interacts directly with metabolic regulators. Thirdly, circadian clock pathways could partially mediate the adjustment of life-history transitions by temperature, as they have previously been linked to the regulation of, for instance, smoltification and spawning in salmonids. The potentially diverged functional roles of circadian clock genes are of high interest in this respect.

Arctic char is known for its high phenotypic plasticity (Saether *et al.* 2015), and our study is focused on one sub-Arctic land-locked population, which may show divergent responses from Arctic populations. However, based on similar responses in expression observed in the clock genes in other fishes as well as in a phylogenetically very distant group, plants, it is likely that this response is conserved. In general, high phenotypic plasticity can contribute significantly to local adaptation, thereby promoting species persistence in heterogenous environments (Aubin-Horth & Renn 2009; Dayan *et al.* 2015; Morris *et al.* 2014). In future studies, its role in the biological clocks of fish in relation to thermal adaptation should also be addressed.

Data availability

Sequence data: All quality-trimmed reads used in this study are available for download at the Short Read Archive (study accession SRP068854). The Transcriptome Shotgun Assembly project has been deposited at DDBJ/EMBL/GenBank under the accession GEKT00000000. The version described in this paper is the first version, GEKT01000000.

Filtered read count data and annotations are available in Figshare (read counts DOI 10.6084/m9.figshare.5662489, annotations DOI 10.6084/m9.figshare.5662741).

Author contributions

Conceptualization: JMP, MN, EHL, KA. Investigation: JMP, KA, ML, MK, KI. Formal analysis: JMP, EHL. Resources: MN, IK, ES. Writing –Original draft: JMP. Writing –Review and editing: JMP, EHL, KA, MN, MK, ML, KI, ES. Visualization: JMP. Supervision: EHL, MN, KA. Funding acquisition: MN, JMP, IK, ES, KA.

References

Akhtar, R.A., Reddy, A.B., Maywood, E.S., Clayton, J. D., King, V. M., Smith, A. G., Gant, T. W., Hastings, M. H., Kyriacou, C. P. (2002) Circadian cycling of the mouse liver transcriptome, as revealed by cDNA microarray, is driven by the suprachiasmatic nucleus. *Curr. Biol.* **12**, 540-550.

Anttila, K., Lewis, M., Prokkola, J.M., Kanerva, M., Seppänen, E., Kolari, I., Nikinmaa, M. (2015) Warm acclimation and oxygen depletion induce species-specific responses in salmonids. *J. Exp. Biol.* **218**, 1471-1477.

Aubin-Horth, N., Renn, S.C.P. (2009) Genomic reaction norms: using integrative biology to understand molecular mechanisms of phenotypic plasticity. *Mol. Ecol.* **18**, 3763-3780.

Belinky, F., Nativ. N., Stelzer, G., Zimmerman, S., Iny Stein, T., Safran, M., Lancet, D. (2015) PathCards: multi-source consolidation of human biological pathways. Database **2015**, bav006.

Bieniawska, Z., Espinoza, C., Schlereth, A., Sulpice, R., Hincha, D. K., Hannah, M. A. (2008) Disruption of the Arabidopsis circadian clock is responsible for extensive variation in the cold-responsive transcriptome. *Plant Physiol* **147**, 263-279.

Brown, F.A., Webb, H.M. (1948) Temperature relations of an endogenous daily rhythmicity in the Fiddler crab, Uca. *Physiological Zoology* **21**, 371-381.

Cowan, M., Azpeleta, C., López‑ Olmeda, J.F. (2017) Rhythms in the endocrine system of fish: a review. *J. Comp. Physiol. B.,* **187**, 1057-1089.

Davidson, N.M., Oshlack, A. (2014) Corset: enabling differential gene expression analysis for *de novo* assembled transcriptomes. *Genome Biol.* **15**.

Dayan, D.I., Crawford, D.L., Oleksiak, M.F. (2015) Phenotypic plasticity in gene expression contributes to divergence of locally adapted populations of *Fundulus heteroclitus*. *Mol. Ecol.* **24**, 3345-3359.

Doherty, C.J., Kay, S.A. (2010) Circadian control of global gene expression patterns. *Annu. Rev. Genet.* **44**, 419-444.

Falcón, J., Besseau, L., Fuentès, M., Sauzet, S., Magnanou, E., Boeuf, G. (2009) Structural and functional evolution of the pineal melatonin system in vertebrates. *Ann. N Y Acad. Sci.* **1163**, 101-111.

Grabherr, M.G., Haas, B.J., Yassour, M., Levin, J. Z., Thompson, D. A., Amit, I., Adiconis, X., Fan, L., Raychowdhury, R., Zeng, Q. *et al.* (2011) Full-length transcriptome assembly from RNA-Seq data without a reference genome. *Nature Biotechnol.* **29**, 644-652.

Hastings, J.W., Sweeney, B.M. (1957) On the mechanisms of temperature independence in a biological clock. *Proc. Natl. Acad. Sci. U. S. A.* **43**, 804-811.

Idda, M.L., Bertolucci, C., Vallone, D., Gothilf, Y., Sanchez-Vazquez, F. J., Foulkes, N. S. (2012) Circadian clocks: lessons from fish. *Prog. brain res.* **199**, 41-57.

Jeuthe, H., Brannas, E., Nilsson, J. (2015) Thermal stress in Arctic charr *Salvelinus alpinus* broodstock: a 28 year case study. *J. Fish Biol.* **86**, 1139-1152.

Johnsen, A., Fidler, A.E., Kuhn, S., Carter, K. L., Hoffmann, A., Barr, I. R., Biard, C., Charmantier, A. Eens, M., Korsten, P. (2007) Avian Clock gene polymorphism: evidence for a latitudinal cline in allele frequencies. *Mol. Ecol.* **16**, 4867-4880.

Jorgensen, E.H., Johnsen, H.K. (2014) Rhythmic life of the Arctic charr: Adaptations to life at the edge. *Mar. Genomics* **14**, 71-81.

Kidd, P.B., Young, M.W., Siggia, E.D. (2015) Temperature compensation and temperature sensation in the circadian clock. *Proc. Natl. Acad. Sci. U. S. A.* **112**, 6284-6292.

Lahiri, K., Vallone, D., Gondi, S.B., Santoriello, C., Dickmeis, T., Foulkes, N. S. (2005) Temperature regulates transcription in the zebrafish circadian clock. *PLoS Biol.* **3**, 2005-2016.

Lahiri, K., Froehlich, N., Heyd, A., Foulkes, N.S., Vallone, D. (2014) Developmental stage-specific regulation of the circadian clock by temperature in zebrafish. *Biomed Res. Int.* **2014**, 930308.

Langfelder, P., Horvath, S. (2008) WGCNA: an R package for weighted correlation network analysis. *BMC Bioinformatics* **9**, 559.

Law, C.W., Chen, Y., Shi, W., Smyth, G.K. (2014) voom: precision weights unlock linear model analysis tools for RNA-seq read counts. *Genome Biol.* **15**.

Leder, E.H., Danzmann, R.G., Ferguson, M.M. (2006) The candidate gene, Clock, localizes to a strong spawning time quantitative trait locus region in rainbow trout. *J. Hered.* **97**, 74-80.

Lopez-Olmeda, J.F., Sanchez-Vazquez, F.J. (2009) Zebrafish temperature selection and synchronization of locomotor activity circadian rhythm to ahemeral cycles of light and temperature. *Chronobiol. Int.* **26**, 200-218.

Lowrey, P.L., Takahashi, J.S. (2004) Mammalian circadian biology: Elucidating genome-wide levels of temporal organization. *Annu. Rev. Genomics Hum. Genet.* **5**, 407-441.

Macqueen, D.J., Johnston, I.A. (2014) A well-constrained estimate for the timing of the salmonid whole genome duplication reveals major decoupling from species diversification. *Proc. Biol. Sci.* **281**.

Martinocatt, S., Ort, D.R. (1992) Low temperature interrupts circadian regulation of transcriptional activity in chilling-sensitive plants. *Proc. Natl. Acad. Sci. U. S. A,* **89**, 3731-3735.

Marshall, J., Armour, K.C., Scott, J.R., Kostov, Y., Hausmann, U., Ferreira, D., Shepherd, T. G., Bitz, C. M. (2014) The ocean's role in polar climate change: asymmetric Arctic and Antarctic responses to greenhouse gas and ozone forcing. *Philos. Trans. A Math. Phys. Eng. Sci.* **372:** 20130040**.**

Mizuno, T., Nomoto, Y., Oka, H. Kitayama, M., Takeuchi, A., Tsubouchi, M., Yamashino, T. (2014) Ambient temperature signal feeds into the circadian clock transcriptional circuitry through the EC night-time repressor in *Arabidopsis thaliana. Plant Cell Physiol.* **55**, 958-976.

Morris, M.R.J., Richard, R., Leder, E.H., Barrett, R. D. H., Aubin-Horth, N., Rogers, S. M. (2014) Gene expression plasticity evolves in response to colonization of freshwater lakes in threespine stickleback. *Mol. Ecol.* **23**, 3226-3240.

Odom, D.T., Zizlsperger, N., Gordon, D.B., Bell, G. W., Rinaldi, N. J., Murray, H. L., Volkert, T. L., Schreiber, J., Rolfe, P. A., Gifford, D. K. *et al*. (2004) Control of pancreas and liver gene expression by HNF transcription factors. *Science*. **303**, 1378-1381.

Oishi, K., Itoh, N. (2013) Disrupted daily light-dark cycle induces the expression of hepatic gluconeogenic regulatory genes and hyperglycemia with glucose intolerance in mice. *Biochem. Biophys. Res. Commun*. **432**,111-115.

O'Malley, K.G., Banks, M.A. (2008) A latitudinal cline in the Chinook salmon (*Oncorhynchus tshawytscha*) Clock gene: evidence for selection on PolyQ length variants. *Proc. Biol. Sci.* **275**, 2813-2821.

Paibomesai, M.I., Moghadam, H.K., Ferguson, M.M., Danzmann, R.G. (2010) Clock genes and their genomic distributions in three species of salmonid fishes: Associations with genes regulating sexual maturation and cell cycling. *BMC res. notes* **3**, 215-215.

Panda, S., Antoch, M.P., Miller, B.H. Su, A. I., Schook, A. B., Straume, M., Schultz, P. G., Kay, S. A., Takahashi, J. S., Hogenesch, J. B. (2002) Coordinated transcription of key pathways in the mouse by the circadian clock. *Cell* **109**, 307-320.

Penney, C.M., Nash, G.W., Gamperl, A.K. (2014) Cardiorespiratory responses of seawater-acclimated adult Arctic char (*Salvelinus alpinus*) and Atlantic salmon (*Salmo salar*) to an acute temperature increase. *Can. J. Fish. Aquat. Sci*. **71**, 1096-1105.

Podrabsky, J.E., Somero, G.N. (2004) Changes in gene expression associated with acclimation to constant temperatures and fluctuating daily temperatures in an annual killifish *Austrofundulus limnaeus*. *J. Exp. Biol.* **207**, 2237-2254.

Porter, M.J.R., Duncan, N., Handeland, S.O., Stefansson, S.O., Bromage, N.R. (2001) Temperature, light intensity and plasma melatonin levels in juvenile Atlantic salmon. *J. Fish Biol.* **58**, 431-438.

Rensing, L., Ruoff, P. (2002) Temperature effect on entrainment, phase shifting, and amplitude of circadian clocks and its molecular bases. *Chronobiol. Int.* **19**, 807-864.

Ritchie, M.E., Phipson, B., Wu, D., Hu, Y., Law, C. W., Shi, W., Smyth, G. K. (2015) limma powers differential expression analyses for RNA-sequencing and microarray studies. *Nucleic Acids Res.* **43**.

Robinson, M.D., Oshlack, A. (2010) A scaling normalization method for differential expression analysis of RNA-seq data. *Genome Biol.* **11,** 25.

Simao, F.A., Waterhouse, R.M., Ioannidis, P., Kriventseva, E.V., Zdobnov, E.M. (2015) BUSCO: assessing genome assembly and annotation completeness with single-copy orthologs. *Bioinformatics* **31**, 3210-3212.

Smyth, G.K. (2005) Limma: Linear models for microarray data. *Bioinformatics and Computational Biology Solution Using R and Bioconductor*, 397-420.

Stevenson, T.J., Visser, M.E., Arnold, W., Barrett, P., Biello, S., Dawson, A., Denlinger, D. L., Dominoni, D., Ebling, F. J., Elton, S. *et al.* (2015) Disrupted seasonal biology impacts health, food security and ecosystems. *Proc. Biol. Sci.* **282**, 20151453.

Strand, J.E.T., Aarseth, J.J., Hanebrekke, T.L., Jorgensen, E.H. (2008) Keeping track of time under ice and snow in a sub-arctic lake: plasma melatonin rhythms in Arctic charr overwintering under natural conditions. *J. Pineal Res.* **44**, 227-233.

Smith-Unna, R., Boursnell, C., Patro, R., Hibberd, J.M., Kelly, S. (2016) TransRate: reference-free quality assessment of *de novo* transcriptome assemblies. *Genome Res.* **26**, 1134-1144.

Saether, B.-S., Siikavuopio, S.I., Jobling, M. (2015) Environmental conditions required for intensive farming of Arctic charr (*Salvelinus alpinus* (L.)) *Hydrobiologia*. DOI: 10.1007/s10750-015-2572-y.

Tauber, E., Kyriacou, C.P. (2008) Genomic approaches for studying biological clocks. *Funct. Ecol.* **22**, 19–29.

Vatine, G., Vallone, D., Gothilf, Y., Foulkes, N.S. (2011) It's time to swim! Zebrafish and the circadian clock. *FEBS Letters* **585**, 1485-1494.

Vallone, D., Frigato, E., Vernesi, C., Foa, A., Foulkes, N. S., Bertolucci, C. (2007) Hypothermia modulates circadian clock gene expression in lizard peripheral tissues. *Am. J. Physiol. Regul. Integr. Comp. Physiol*. **292**, 160-166.

Vera, L.M., Migaud, H. (2016) Hydrogen peroxide treatment in Atlantic salmon induces stress and detoxification response in a daily manner. *Chronobiol. Int*. **33**, 530-542.

Walsh, J.E. (2008) Climate of the arctic marine environment. *Ecol. Appl.* **18**, 3-22.

Warnes, G.R., Bolker, B., Bonebakker, L., Gentleman, R., Huber, W., Liaw, A., Lumley, T., Maechler, M., Magnusson, A., Moeller, S. *et al*. (2016). gplots: Various R Programming Tools for Plotting Data. R package version 3.0.1. https://CRAN.R-project.org/package=gplots

Whitmore, D., Foulkes, N.S. & Sassone-Corsi, P. (2000). Light acts directly on organs and cells in culture to set the vertebrate circadian clock. *Nature* **404**, 87–91.

Wickham, H. (2009) ggplot2: Elegant Graphics for Data Analysis. *Ggplot2: Elegant Graphics for Data Analysis*, 1-212.

Wickham, H. (2011) The Split-Apply-Combine Strategy for Data Analysis. *J Stat. Softw.* **40**, 1-29.

Wood, S., Loudon, A. (2014) Clocks for all seasons: unwinding the roles and mechanisms of circadian and interval timers in the hypothalamus and pituitary. *J. Endocrinol.* **222**, 39-59.

Yoshitane, H., Ozaki, H., Terajima, H., Du, N.-H., Suzuki, Y., Fujimori, T., Kosaka, N., Shimba, S., Sugano, S., Takagi, T., *et al.* (2014) CLOCK-Controlled polyphonic

regulation of circadian rhythms through canonical and noncanonical E-boxes. *Mol. Cell. Biol.* **34**, 1776-1787.

Zachmann, A., Falcon, J., Knijff, S.C.M., Bolliet, V., Ali, M.A. (1992) Effects of photoperiod and temperature on rhythmic melatonin secretion from the pineal organ of the white sucker (*Catostomus commersoni*) *in vitro. Gen. Comp. Endocrinol.* **86**, 26-33.

Tables

Table 1. Summary of genes showing significant temporal variation in Arctic char liver at 15°C.

Direction	Day & Evening	Day & Night	Evening & Night
Increase	1041	473	108
Decrease	679	274	65

Table 2. Members of the super pathway "BMAL1-CLOCK,NPAS2 activates circadian gene expression" that were significantly differentially expressed in the contrasts used in DE analysis (FDR <0.05) or that were found as potential upstream regulators of gene modules. Time refers to contrasts between any two time points at 15°C, Int to the interaction effect of Time and Temperature. Temperature contrasts are abbreviated as Temp = temperature midpoint, Temp1–3 = Temperature contrast at 12:30, 20:30 and 01:30, respectively.

Gene symbol	Contrasts	Assigned upstream regulator to module
ARNTL	Temp1-3, Temp, Time, Int	Turquoise
ARNTL2	Temp3, Temp, Int	
BHLHE40	Time, Temp2, Int	
CARM1	Time, Temp2	
CHD9	Temp2	
CLOCK	Time, Temp3, Temp, Int	Turquoise, Yellow, Green
CPT1A	Temp1, Temp3, Temp	
CREB1	Time, Temp2-3, Temp, Int	Turquoise, Yellow
CREBBP	Temp, Temp2-3, Int	Greenyellow
CRY1	Temp, Temp2-3, Int	
CSNK1D	Time, Temp2-3, Temp, Int	
CTGF	Time, Temp2, Temp, Int	
DBP	Temp1, Temp	Turquoise
EP300	Temp, Temp2-3, Int	Turquoise, Greenyellow
HDAC3	Time	Greenyellow
HELZ2	Temp1-3, Temp, Int	
HIF1A	Temp2-3, Temp	Turquoise, Blue, Yellow, Brown
HIPK2	Temp	Cyan
KAT2B	Temp2, Temp	Cyan
MEF2D	Temp2, Temp, Int	
NAMPT	Temp1, Temp	
NCOA1	Temp3, Temp, Int	Turquoise, Blue, Brown
NCOA6		Turquoise
NCOR1	Time, Temp3, Temp, Int	
NOCT	Temp, Int	
NPAS2		Turquoise, Yellow, Midnightblue
NR1D1	Temp	Turquoise, Greenyellow
NR3C1	Int	Turquoise, Yellow, Greenyellow
PER1	Temp	
PER2	Temp	Cyan
PPARA		Turquoise, Blue, Brown, Midnightblue
PPARGC1A		Turquoise
PPP1CB	Temp	
RORA		Turquoise
RUNX2		Turquoise
RXRA		Turquoise, Blue, Brown
SIK1	Temp, Temp2	
SIRT1	Time, Temp, Int	Turquoise, Magenta
SMARCD3	Temp1, Temp3, Temp	Turquoise
SREBF1	Temp, Temp2	Turquoise
TBL1X		Greenyellow
TEAD3	Temp3	
TBL1XR1	Time, Temp, Int	Greenyellow
UBC	Temp1, Time	

Table 3. Summary of gene modules identified with WGCNA.

Most sign. correlation	Module color	Number of genes
Time	Green	1097
	Yellow	1164
Temperature	Blue	2465
	Brown	1482
	Cyan	60
	Greenyellow	111
	Lightcyan	50
	Magenta	200
	Midnightblue	50
	Turquoise	2961
	Total	9640

Table 4. The number of significantly differentially expressed genes from the midpoint contrast between temperatures, the pairwise contrasts between time points in each temperature, or the interaction of time and temperature overlapping with the members of gene modules from WGCNA. Shown are modules that had a significant correlation with time or temperature.

	Total	Temperature	Time 15°C	Time 8°C	Interaction
blue	808	709	34	0	65
brown	1329	1255	14	6	60
green	431	50	198	0	183
greenyellow	84	80	0	0	4
magenta	49	38	10	0	1
turquoise	3485	1952	519	1	1013
yellow	1145	135	572	5	433

Figures
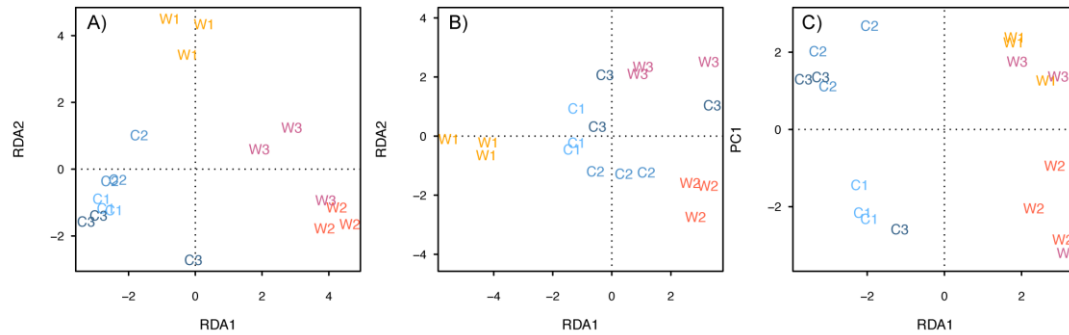
Figure 1. Clustering of samples based on (partial) RDA. Samples collected from warm (W, 15°C) and cold temperature (C, 8°C) during light period (12:30 and 20:30) and dark period (01:30) are indicated by 1, 2 or 3, respectively. A) Both temperature and time used as explanatory variables. The axis eigenvalues are 4,600.5 for RDA1 and 2,585.2 for RDA2. In total 45% of constrained variance explained (adj. $R^2 = 0.22$). B) Time, after conditioning for the effect of temperature, used as explanatory variable. The axis eigenvalues are 1,947.0 for RDA1, and 903.2 for RDA2. 13% of total constrained variance explained (adj. $R^2 = 0.04$). C) Temperature, after conditioning for the effect of time, used as explanatory variable. The axis eigenvalues are 4,052.5 for RDA1, and 2,724.4 for PC1. 18% of constrained variance explained (adj. $R^2 = 0.15$).
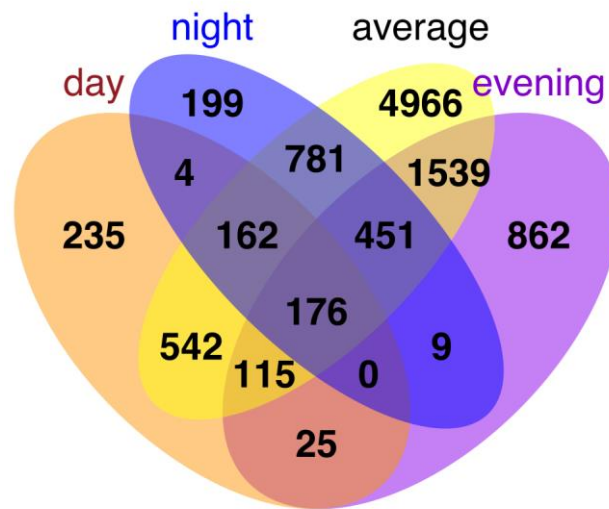
Figure 2. Venn diagram depicting the number of differentially expressed genes at three different time points and in the contrast of temperature midpoint (average).
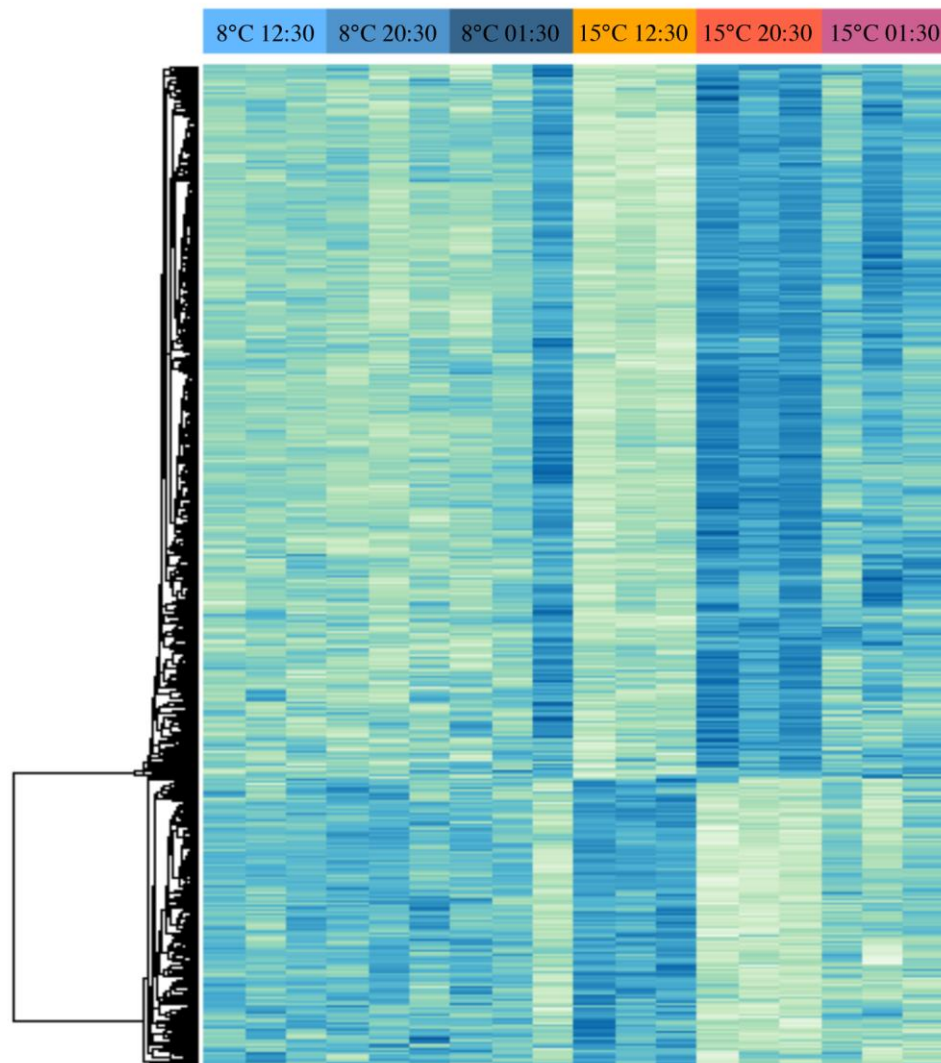
Figure 3. Heatmap of genes in the yellow module that was significantly correlated with time. Samples are grouped by temperature and time point. Genes were clustered by distances based on Pearson correlation coefficients. Lighter colour indicates lower expression; row Z-score scale from –3 (light yellow) to 3 (dark blue).

Supplemental Figures
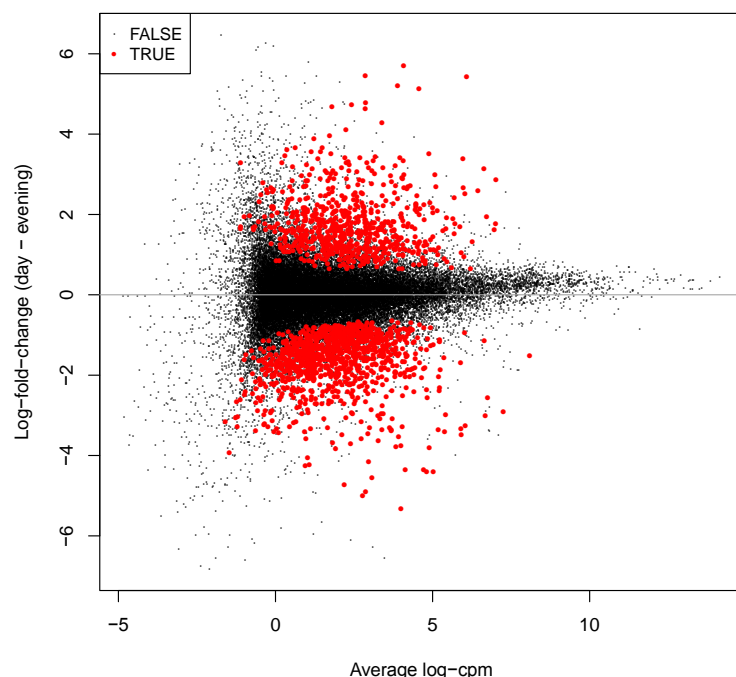
Fig S1. A fitted model MD-plot of the contrast between samples from 20:30 and 12:30 in the warm acclimated fish (N=3). Red dots indicate genes that were considered differentially expressed (FDR <0.05). Mean expression levels are indicated by $\log_2$ counts per million mapped reads (log-cpm).
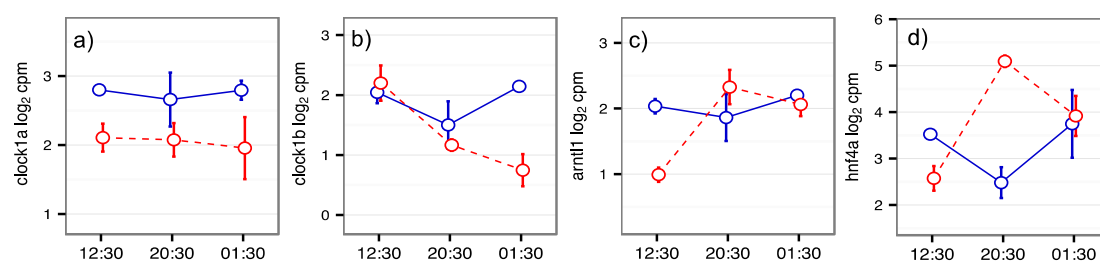

Fig S2. Line plots of selected time and/or temperature responsive genes in male Arctic char liver after one month acclimation at 15°C (red dashed line) or 8°C (blue solid line). Values are mean $\log_2$ counts per million mapped reads (cpm) ± SD. N=3 in each point. Expression levels were not standardized for gene length and therefore are not comparable between genes. Full gene names: a) *circadian locomotor output cycles kaput 1a,* b) *circadian locomotor output cycles kaput 1b,* c) *aryl hydrocarbon receptor nuclear translocator-like protein 1,* d) *hepatocyte nuclear factor 4 alpha.*
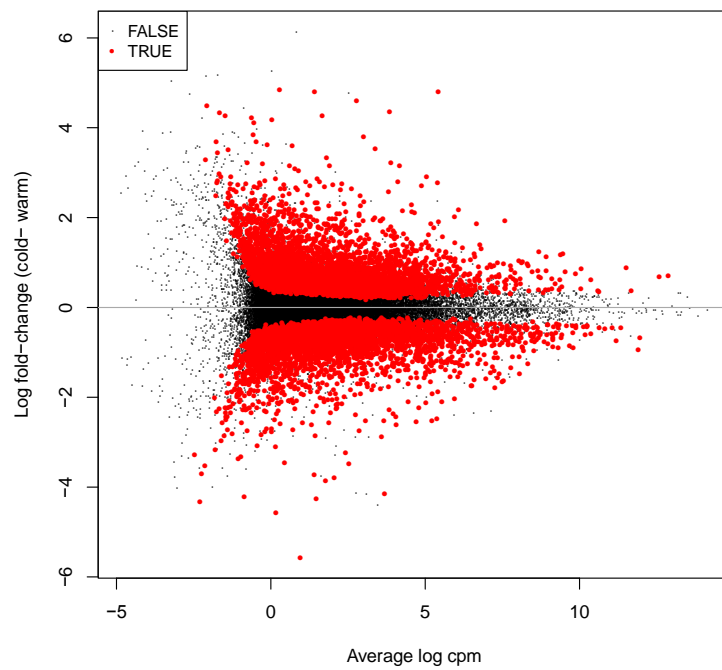
Fig S3. A fitted model MD-plot of the midpoint contrast between samples from the cold (8°C) and warm (15°C) temperatures (N=9). Red dots indicate genes that were considered differentially expressed (FDR <0.05). Expression levels are indicated by $\log_2$ counts per million mapped reads (log-cpm).
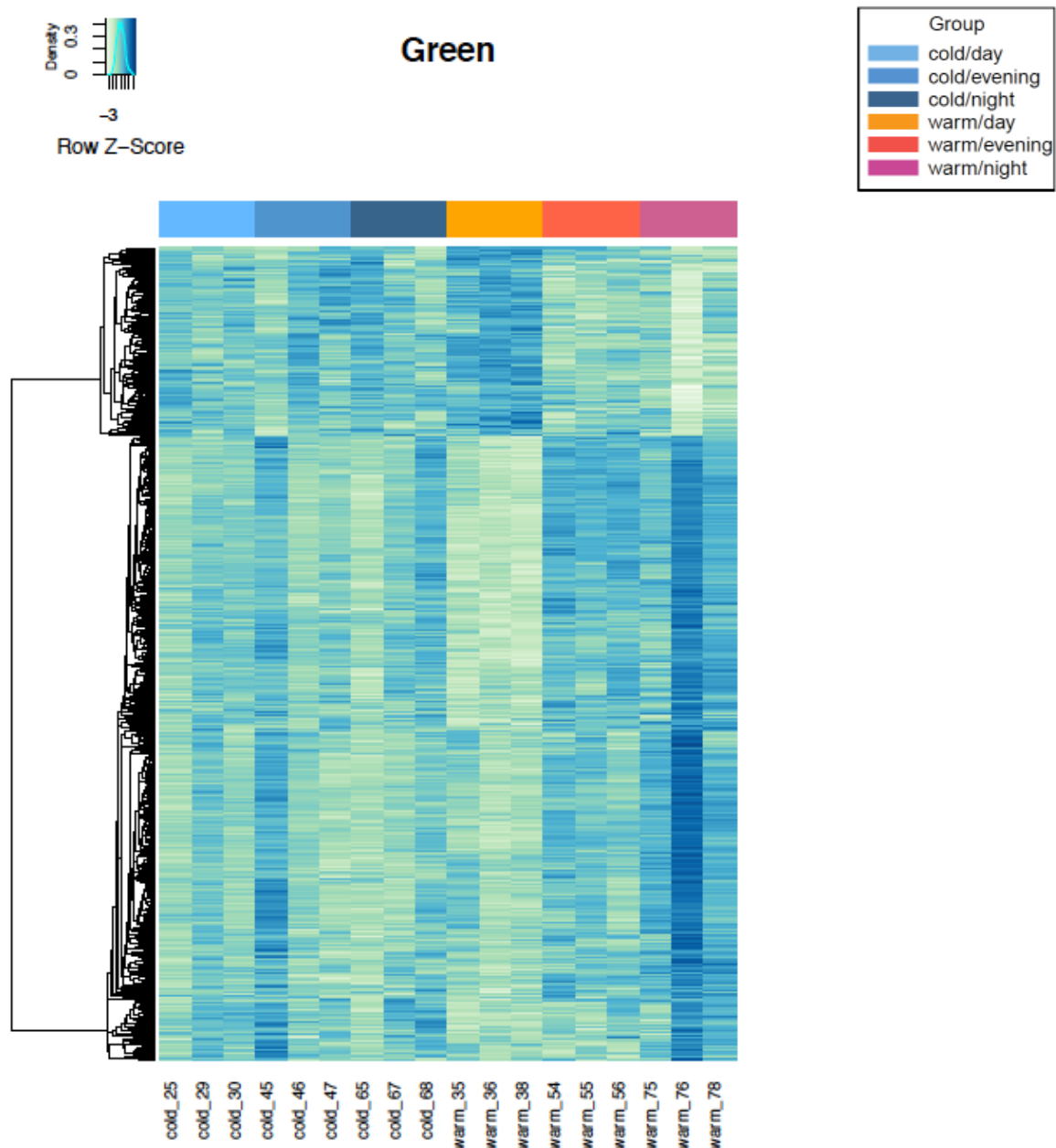
Fig S4. A heatmap showing the clustering of genes from Green module, which was significantly correlated with time in WGCNA. The list of genes belonging to the module is shown in Table S6.
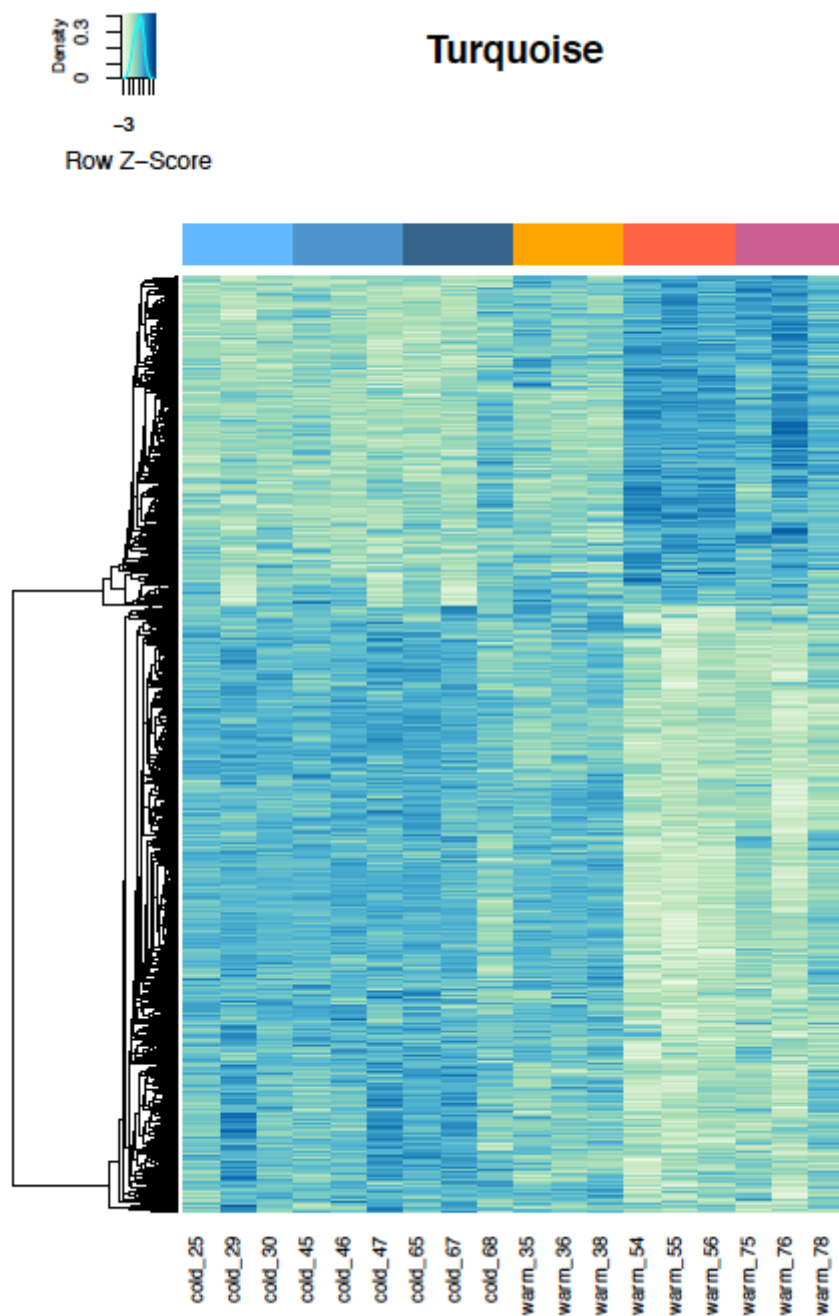
Fig S5. A heatmap showing the clustering of genes from Turquoise module, which was significantly correlated with temperature in WGCNA. Legend for color bar is shown in Fig S4. The list of genes belonging to the module is shown in Table S6.
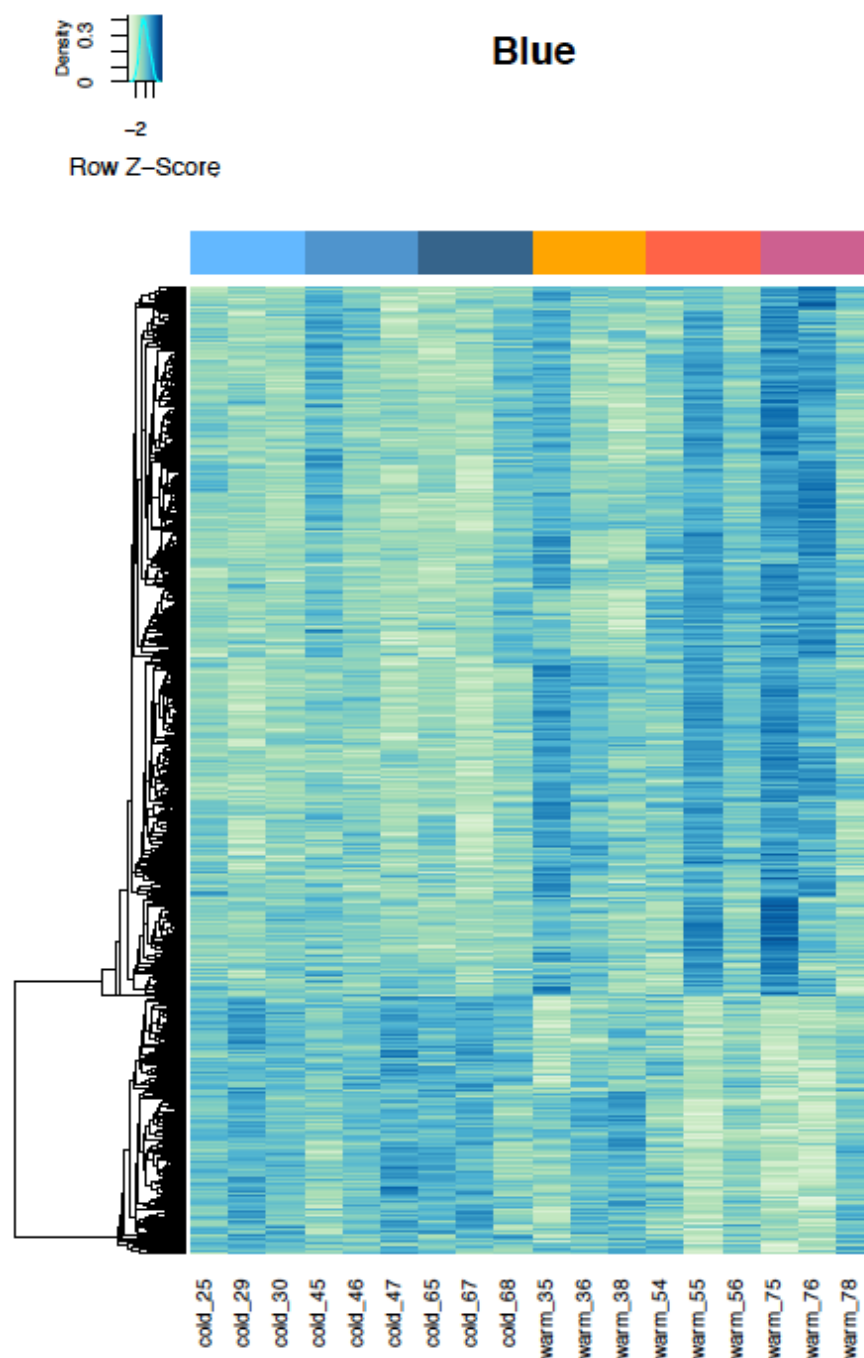
Fig S6. A heatmap showing the clustering of genes from Blue module, which was significantly correlated with temperature in WGCNA. Legend for color bar is shown in Fig S4. The list of genes belonging to the module is shown in Table S6.
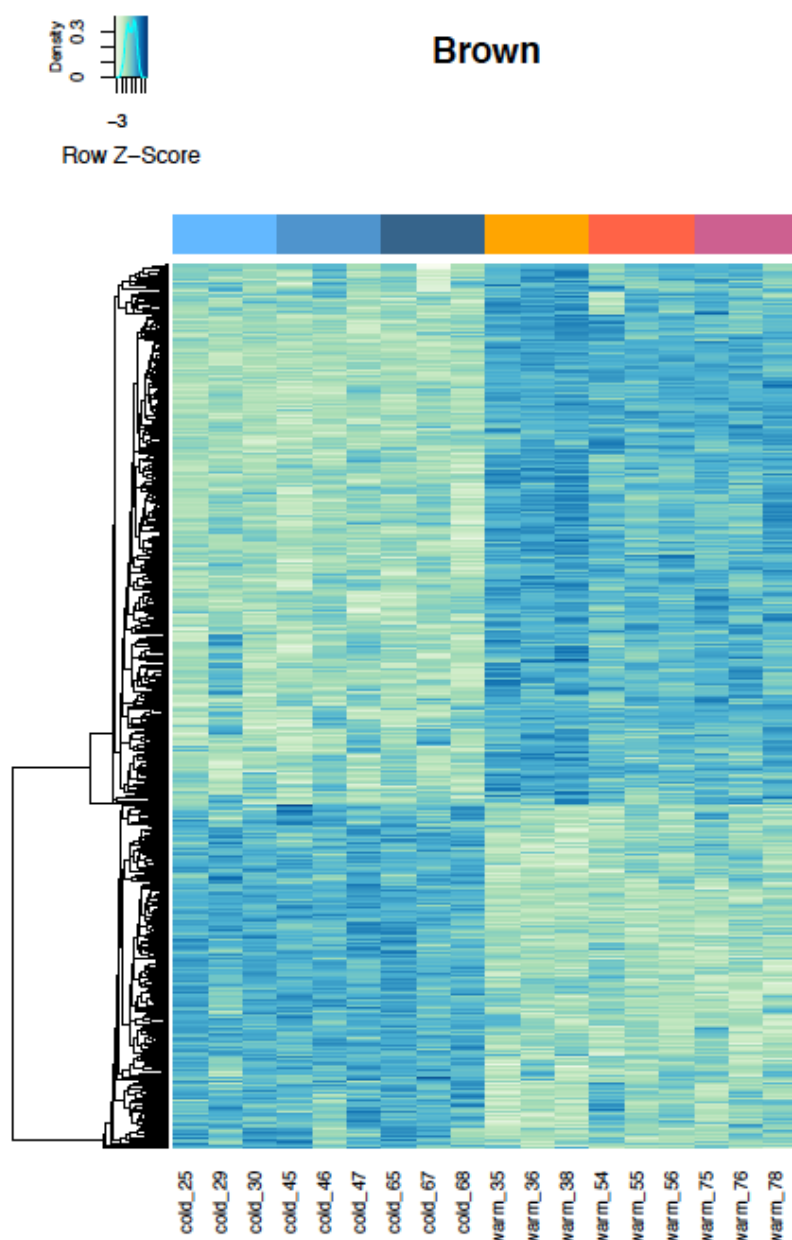
Fig S7. A heatmap showing genes belonging to the brown module, which was significantly correlated with temperature in WGCNA. Legend for the color bar is shown in Fig S4. The list of genes belonging to the module is shown in Table S6.

Supplemental Experimental Procedures

Library preparation and RNA-sequencing at BGI
TruSeq RNA Sample Prep Kit v2 (Illumina) was used to construct libraries from 200 ng total RNA sample enriched for mRNA using oligo-dT beads. After RNA fragmentation, first-strand cDNA was generated by First Strand Master Mix and Super Script II (Invitrogen) reverse transcription (Reaction conditions: 25°C for 10 min; 42°C for 50 min; 70°C for 15 min). The products were purified with Agencourt RNAClean XP Beads (Agencourt). Second strand cDNA synthesis was done with Second Strand Master Mix and dNTP mix at 16°C for 1h. The cDNA was combined with End Repair Mix, incubated at 30°C for 30 min and purified with Ampure XP Beads (Agencourt). PolyA-tails were added (A-Tailing Mix) and samples incubated at 37°C for 30 min. RNA Index Adapter and Ligation Mix were added to

the Adenylated 3'Ends DNA and samples incubated at 30°C for 10 min. The end-repaired DNA was purified with Ampure XP Beads. To perform strand-specific sequencing, the second strand of cDNA was digested using Uracil-N-Glycosylase enzyme and incubation at 37°C for 10 min, after which the samples were purified with Ampure XP Beads. Several rounds of PCR amplification with PCR Primer Cocktail and PCR Master Mix were performed to enrich the cDNA fragments. The PCR products were purified with Ampure XP Beads. The libraries were assessed for quality and quantity using two methods: checking the distribution of the fragments size using the Agilent 2100 bioanalyzer instrument (Agilent DNA 1000 Reagents) and quantifying the library using real-time quantitative PCR (qPCR) with a TaqMan Probe. The quality-checked libraries were amplified on cBot to generate the cluster on the flow cell (TruSeq PE Cluster Kit V3–cBot–HS, Illumina). The amplified flowcell was sequenced paired end on the HiSeq 2000 System (TruSeq SBS KIT-HS V3, Illumina) using 101 bp read length. Prior to sequencing, all samples were pooled and distributed across four lanes. Additional sequencing for the assembly construction was performed from the same samples pooled across two lanes.

Details on *de novo* transcriptome assembly
The assembly and downstream analyses were conducted using computing resources from the IT Centre for Science, Espoo, Finland, (www.csc.fi). Due to challenges posed by accurately determining transcripts in a pseudotetraploid species, the transcriptome assembly was built in three steps. At first, the data from all individuals was combined and assembled using Trinity software, v. 2.0.6 (Grabherr *et al.* 2011). The samples were aligned back to the transcriptome using Bowtie2 v.2.2.5 (Langmead & Salzberg 2012) allowing for a maximum of 40 multiple alignments when no unique alignment could be determined. Read counts per gene were analyzed with Corset software v.1.03, which clusters transcripts based on sequence similarity and expression levels (Davidson & Oshlack 2013). Read count data was used to determine which samples covered the most variation in expression by determining the distance of samples based on all transcripts using DeSeq2 package (Love *et al.* 2014) in R (R Core Team, 2014). The distance was greatest between samples from cold acclimation and the evening time point from the warm acclimated fish. Thus, the sample with the highest number of reads from both of these groups was chosen for the generation of the next assembly in order to reduce redundancy caused by using a large number of individuals. The second assembly was constructed using Trinity on trimmed reads obtained from two samples (in total approx. 170 M read pairs) using minimum kmer coverage of five reads and minimum kmer length of 30 bp.

To improve the assembly, the samples used to generate the second assembly were aligned to the transcripts generated using Bowtie2, and reads that were not concordantly aligned were used to generate a third assembly using Trinity. Finally, a BLAST search between the second and third assembly was used to remove the redundant transcripts, and the transcripts from third assembly that had less than 98 % similarity to those present in the second assembly and were longer than 100 bp were appended to the second assembly. Assembly quality was determined by the number of transcripts identified, rate of unique/multiple mapping reads, number of hits to Uniprot Swissprot database using BLASTx, the number of full-length hits from predicted open reading frames (ORFs) to Uniprot Swissprot database using BLASTp and using BUSCO, which estimates the completeness using universal single copy orthologs with the dataset for vertebrates (Simao *et al.* 2015). Additionally, the cDNA sequences from a set of 20 conserved paralogous genes in salmonids were compared to the final assembly using BLASTn.

Options of software used during *de novo* assembly

Trimmomatic
LEADING:5 TRAILING:5 SLIDINGWINDOW:4:15 MINLEN:36

Trinity
Assembly from two samples

--seqType fq --max_memory 96G --left all_25_pr.fq,all_56_pr.fq --right all_25_pf.fq,all_56_pf.fq --SS_lib_type RF --normalize_reads --min_kmer_cov 5 --KMER_SIZE 30

Assembly from unmapped reads

--seqType fq --max_memory 96G --left 25_unmapped.1.fq,56_unmapped.1.fq\
 --right 25_unmapped.2.fq,56_unmapped.2.fq --SS_lib_type RF --min_kmer_cov 2 --KMER_SIZE 30

Bowtie2

--phred64 --end-to-end -k 40 -D 20 --fr --no-mixed --no-discordant --score-min L,-0.1,-0.1 --no-unal

Supplemental References

Davidson NM, Oshlack A (2014) Corset: enabling differential gene expression analysis for de novo assembled transcriptomes. *Genome Biology* **15**.

Grabherr MG, Haas BJ, Yassour M *et al*. (2011) Full-length transcriptome assembly from RNA-Seq data without a reference genome. *Nature Biotechnology* **29**, 644-652.

Langmead B, Salzberg SL (2012) Fast gapped-read alignment with Bowtie 2. *Nature Methods* **9**, 357-359.

Love MI, Huber W, Anders S (2014) Moderated estimation of fold change and dispersion for RNA-seq data with DESeq2. *Genome Biology* **15**.

Simao FA, Waterhouse RM, Ioannidis P, Kriventseva EV, Zdobnov EM (2015) BUSCO: assessing genome assembly and annotation completeness with single-copy orthologs. *Bioinformatics* **31**, 3210-3212.

Table S1. Results of BLASTn comparing known conserved cDNA sequences of paralogous gene pairs in salmonids to the *de novo* Arctic char transcriptome assembly. Different cluster IDs indicates that the paralogs were matching to separate contigs in the transcriptome.

Click here to Download Table S1

Table S2. Linear model results and annotations for the genes (clusters) with significant pairwise changes between three time points (12:30 and 20:30 and 01:30) in Arctic char acclimated at 15°C for one month. Log$_2$ fold change (Log2FC) >0 indicates higher expression at the earlier time point. T-test values for each contrast are followed by unadjusted P-values (FDR <0.05 based on limma "global" option was used to filter results). Empty cells indicate the gene was not differentially expressed in a given contrast. Annotations for predicted open reading frame peptide sequences were prioritized with zebrafish protein sequences, predicted Atlantic salmon protein sequences and NCBI nr-database (genbank_id). Additionally, gene symbols were combined from human, zebrafish, salmon and NCBI orthologs when available.

Click here to Download Table S2

Table S3. Linear model results and annotations for the genes (clusters) with significant pairwise changes between three time points (12:30 and 20:30 and 01:30) in Arctic char acclimated at 8°C for one month. Log$_2$ fold change (Log2FC) >0 indicates higher expression at the earlier time point. T-test values for each contrast are followed by unadjusted P-values (FDR <0.05 based on limma "global" option was used to filter results). Empty cells indicate the gene was not differentially expressed in a given contrast. Annotations for predicted open reading frame peptide sequences were prioritized with zebrafish protein sequences, predicted Atlantic salmon protein sequences and NCBI nr-database (genbank_id). Additionally, gene symbols were combined from human, zebrafish, salmon and NCBI orthologs when available.

Click here to Download Table S3

Table S4. Linear model results and annotations for the genes (clusters) with a significant time-temperature interaction effect. P-values were adjusted for multiple comparisons using Benjamini-Hochberg method (FDR <0.05). Annotations for predicted open reading frame peptide sequences were prioritized with zebrafish protein sequences, predicted Atlantic salmon protein sequences and NCBI nr-database (genbank_id). The counts of transcripts within genes are identical because read counts were obtained at the gene level (annotations were retrieved for transcripts). Additionally, gene symbols were combined from human, zebrafish, salmon and NCBI orthologs when available.

Click here to Download Table S4

Table S5. Linear model results and annotations for the genes (clusters) with a significant temperature midpoint difference (across three time points at 8°C vs. 15°C). Log$_2$ fold change >0 indicates expression was higher at the low temperature. P-values were adjusted for multiple comparisons using Benjamini-Hochberg method (FDR <0.05). Annotations for predicted open reading frame peptide sequences were prioritized with zebrafish protein sequences, predicted Atlantic salmon protein sequences and NCBI nr-database (genbank_id). The counts of transcripts within genes are identical because read counts were obtained at the gene level (annotations were retrieved for transcripts). Additionally, gene symbols were combined from human, zebrafish, salmon and NCBI orthologs when available.

Click here to Download Table S5

Table S6. Modules of genes significantly correlated with sampling time or temperature in Arctic char liver. GS = gene significance, p.GS= P-value of gene significance. Gene symbol = annotation.

Click here to Download Table S6

Table S7. Prokkola et al.

Putative upstream regulators with target genes from Ingenuity Pathway Analysis for gene modules identified with WGCNA in Arctic char liver tissue. Each sheet contains the results for one module.

Click here to Download Table S7

Supplemental Information 2

Click here to Download Supplemental Information 2